第 27 卷第 6 期
2011 年 6 月

无 机 化 学 学 报
CHINESE JOURNAL OF INORGANIC CHEMISTRY

Vol.27 No.6
1171-1176

LaF_3 纳米片和棒束的选择性合成及表征

孙同明　石玉军　汤艳峰　王　淼*
(南通大学化学化工学院,南通　226019)

摘要：室温条件下,以简单的液相法,通过改变氟源 $NaBF_4$ 和 K_2SiF_6,制得不同形貌的 LaF_3 纳米晶(片及棒束)。X 射线衍射(XRD)结果显示所得的 2 种不同形貌的产物均为结晶良好的六方相 LaF_3。场发射扫描电子显微镜(FE-SEM)、透射电子显微镜(TEM)结果表明由 $NaBF_4$ 制得大量均匀、厚度约为 20 nm 的六边形纳米片,而由 K_2SiF_6 得到平均直径约 200 nm、长度约 400 nm 的棒束。本文详细讨论了氟源种类、反应时间、温度、反应物比例等反应参数对产物 LaF_3 形貌的影响。提出了可能的反应机理并进一步研究了掺杂产物 LaF_3:Eu^{3+}及 LaF_3:Tb^{3+}在室温下的荧光性质。

关键词：稀土氟化物；纳米材料；溶液法；掺杂；荧光
中图分类号：O614.33+1；O613.41　　**文献标识码**：A　　**文章编号**：1001-4861(2011)06-1171-06

Selective Synthesis and Characterization of LaF_3 Nanoplates and Bundles

SUN Tong-Ming　SHI Yu-Jun　TANG Yan-Feng　WANG Miao*
(*School of Chemistry and Chemical Engineering, Nantong University, Nantong, Jiangsu* 226019, *China*)

Abstract: At room temperature, LaF_3 nanocrystals with different morphologies (plates and bundles) have been successfully fabricated via a simple solution route by varying the fluoride source ($NaBF_4$ and K_2SiF_6). X-ray powder diffraction (XRD) results indicate that all the as-prepared different morphological LaF_3 products have hexagonal structure and high crystallinity. Field emission scanning electron microscopy (FE-SEM) and transmission electron microscopy (TEM) results show that large-scale and uniform hexagonal nanoplates with thickness about 20 nm can be easily synthesized from $NaBF_4$, while bundles with diameter of 200 nm and length about 400 nm have been prepared from K_2SiF_6. Some reaction parameters (fluoride source, reaction time, temperature and molar ratio of reactants) have been systematically investigated during the process of obtaining different morphological LaF_3. Furthermore, a possible reaction mechanism for the growth of LaF_3 is proposed and the room temperature photoluminescent properties of LaF_3:Eu^{3+} and LaF_3:Tb^{3+} crystals have been measured.

Key words: rare earth fluorides; nanomaterials; solution route; dope; photoluminescence

0 Introduction

Binary lanthanide fluoride (LnF_3) materials, a kind of important rare-earth based compound, has attracted increasing attention in modern materials due to their many potential applications in optics, biological labeling[1-4]. Among these fluorides, LaF_3 nano- and microstructures have recently stimulated broad research interests since it can be used as a host crystal for lanthanide-doped phosphors with interesting down/up conversion luminescent properties. Numerous efforts have been devoted to the exploration of LaF_3 and Ln^{3+}-

收稿日期:2011-01-05。收修改稿日期:2011-03-02。
国家自然科学基金(No.20906052),江苏省自然科学基金(No.BK2010281),南通市科技计划(No.K2008001),南通大学校级课题(No.09ZY003)资助项目。
*通讯联系人。E-mail:wangmiao@ntu.edu.cn

doped LaF_3 with multiform structures and morphologies. Ln^{3+}-doped LaF_3 nanoparticles[1-3], spheres[4], triangular nanoplates [5], hexagon-shaped nanoplates[6-9], nanodisks [10], nanorod [11] and nanowires [12] have been reported in literatures. A variety of simple and efficient approaches have been employed to fabricate these materials, including co-precipitation, single-source precursor (SSP) strategy, hydrothermal and polyol route[1-13].

Recently tetrafluroborate complexes ($NaBF_4$, NH_4BF_4 or KBF_4) have been used to prepare rare-earth fluorides with multiform morphologies. YF_3 hollow peanuts[14], SmF_3 microplates[15], EuF_3 nanospindles & nanodisks[16] have been successfully prepared in our previous work. Employing trisodium citrate (Cit^{3-}) as organic additive, Lin and his coworkers have successfully prepared rare-earth fluoride ReF_3 (Re=La to Lu) nano-/microcrystals from $NaBF_4$ under hydrothermal condition[17]. By employing KBF_4 as fluoride source, Cao have prepared a series of different morphological rare-earth fluoride nanoparticles with sonochemical route, including EuF_3 nanoflowers[18] and CeF_3 nanodisks[19]. However, to the best of our knowledge, few studies have focused on the synthesis of highly mono-dispersed LaF_3 nanocrystals by complex fluorides at room temperature. Herein, we present a simple solution route at room temperature to synthesize different morphological LaF_3. Two fluoride sources, $NaBF_4$ and K_2SiF_6 have been used to prepare plates and bundle-like LaF_3. It is found that fluoride source, molar ratio of reactants and reaction time play crucial roles in the formation of different morphologies of products. Furthermore, the room-temperature photoluminescent properties of Eu^{3+} or Tb^{3+} doped LaF_3 crystals have been investigated.

1 Experimental

1.1 Preparation

Lanthanide oxides Ln_2O_3 (Ln=La, Eu, 99.99 %) and Tb_4O_7 (99.99 %) were purchased from Shanghai Yue Long New Materials Corporation. $NaBF_4$ (A.R.) and K_2SiF_6 (A.R.) were purchased from Shanghai Chemical Reagent Corporation. The lanthanide nitrate $Ln(NO_3)_3 \cdot 6H_2O$ (Ln =La, Eu, Tb) precursors were prepared by dissolving the corresponding lanthanide oxides in a diluted nitric acid solution, and the water in the solutions was evaporated by heating. A typical procedure for the preparation of LaF_3 is given below. 1.0 mmol $La(NO_3)_3 \cdot 6H_2O$ and a certain amount of fluorides (0.75 mmol $NaBF_4$ or 0.5 mmol K_2SiF_6) were dissolved in 25 mL of distilled water in a 50 mL plastic flask, and the solution was stirred at room temperature for a fixed reaction period. The resulting white solid precipitates were collected and washed several times with distilled water and ethanol in an ultrasonic bath. The final products were dried at 70 ℃ for 3 h. Tb^{3+} or Eu^{3+} doped LaF_3 samples were prepared by the same procedure except for additional 5 mol% (total molar ratio) $Eu(NO_3)_3 \cdot 6H_2O$ or $Tb(NO_3)_3 \cdot 6H_2O$ into $La(NO_3)_3 \cdot 6H_2O$ solution at the initial stage.

1.2 Materials characterization

The crystalline phases of the products were analyzed by XRD on a Shimadzu XRD-6000 powder X-ray diffractometer (Cu $K\alpha$ radiation λ=0.154 18 nm), employing a scanning rate of 4.00° · min^{-1}, in the 2θ range from 10° to 80° . The operation voltage and current were maintained at 40 kV and 30 mA, respectively. The sizes and morphologies of the resulting products were studied by transmission electron microscopy (TEM, TECNAI F20S-TWIN) and field emission scanning electron microscopy (FE-SEM, HITACHI S-4800). The luminescent spectra of the solid samples were recorded on HITACHI F-4500 spectrophotometer at room temperature.

2 Results and discussion

2.1 Structure characterization

When the reaction time fixed at 6 h, the XRD patterns of the as-obtained products from $NaBF_4$ or K_2SiF_6 have been measured. Fig.1a shows the XRD of the sample obtained with a molar ratio of $La(NO_3)_3 \cdot 6H_2O$ to $NaBF_4$ as 1∶0.75 and 1∶2, respectively. All diffraction peaks can be easily indexed to pure and hexagonal crystalline phase LaF_3 with a P3c1 space group, which are in agreement with values of the standard card (PDF No.32-0483). However, the diffraction peaks obtained from $n_{La^{3+}}/n_{BF_4^-}$ as 1∶2 are much sharper than the product obtained from 1∶0.75.

According to Scherrer equation, it is clearly indicated that the product crystallinity improved and particle size increased with the increasing of molar ratio of starting materials. K_2SiF_6, another inorganic complex fluoride, is also used as fluoride source to synthesize LaF_3. LaF_3 is prepared when setting molar ratio of $n_{La^{3+}}/n_{SiF_6^{2-}}$ as 1:0.5 or 1:2. Fig.1b shows the XRD pattern of the as-synthesized product obtained after 6 h of reaction time. All diffraction peaks of the product are perfectly indexed to the hexagonal phase of LaF_3 (PDF No.32-0483). No peak of impurities is observed, confirming the formation of pure LaF_3. From Fig.1, it clearly reveals that the varying molar ratio of $n_{La^{3+}}/n_{BF_4^-}$ and $n_{La^{3+}}/n_{SiF_6^{2-}}$ has no great effect on the crystalline phase, no phase transition occurs.

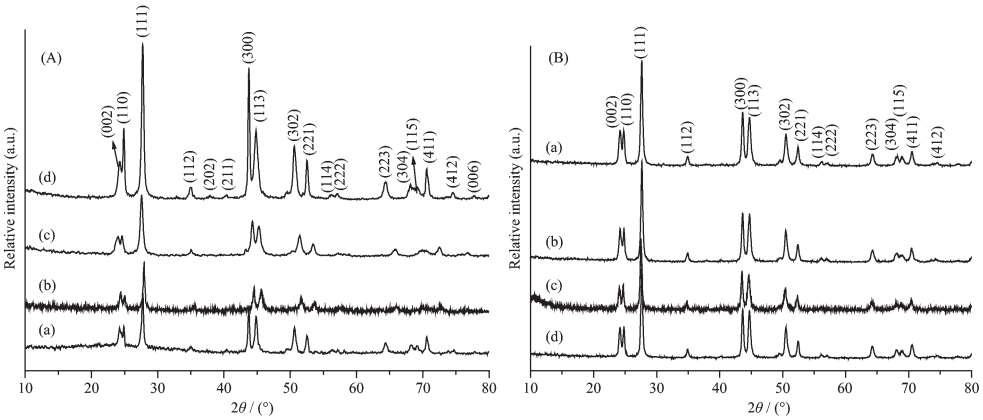

(A) (a) $n_{La^{3+}}/n_{BF_4^-}$=1:0.75, (b) $(n_{0.05Eu^{3+}}+n_{0.95La^{3+}})/n_{BF_4^-}$=1:0.75, (c) $(n_{0.05Eu^{3+}}+n_{0.95La^{3+}})/n_{BF_4^-}$=1:0.75, (d) $n_{La^{3+}}/n_{BF_4^-}$=1:2;

(B) (a) $n_{La^{3+}}/n_{SiF_6^{2-}}$=1:0.5, (b) $(n_{0.05Eu^{3+}}+n_{0.95La^{3+}})/n_{SiF_6^{2-}}$=1:0.5, (c) $(n_{0.05Eu^{3+}}+n_{0.95La^{3+}})/n_{SiF_6^{2-}}$=1:0.5, (d)$n_{La^{3+}}/n_{SiF_6^{2-}}$=1:2

Fig.1　XRD patterns for the as-prepared LaF_3 and Tb^{3+} (or Eu^{3+}) doped LaF_3 samples after reaction for 6 h

2.2　Morphology characterization

Fig.2a~b displays the SEM images of the product with the molar ratio of $La(NO_3)_3\cdot 6H_2O$ to $NaBF_4$ of 1:0.75 after reaction for 6 h. The low magnification SEM image (Fig.2a) indicates that the as-synthesized sample consists of a large quantity of uniform hexagonal nanoplates with well-defined crystallographic facets. The magnified SEM image (Fig.2b) shows that the general morphology of the as-prepared LaF_3 consists of highly dispersed hexagonal plates with an average edge

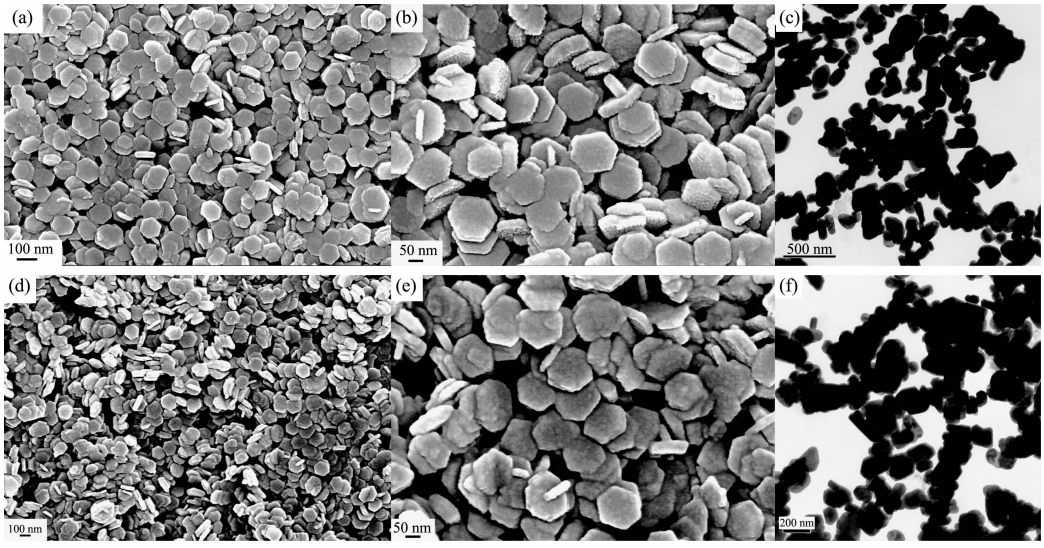

Fig.2　SEM and TEM images of the LaF_3 prepared from $NaBF_4$ ($n_{La^{3+}}/n_{BF_4^-}$=1:0.75) in different periods of time: a~c (6 h), d~f (12 h)

length of 200 nm and a thickness of 20 nm. Fig.2c shows the TEM image of LaF_3 nanoplates. Some nanoplates appear rod-like because they do not lie tightly on the TEM grid and either lie flat on the faces or stand on the edges. When the reaction time is increased to 12 h, while other reaction conditions are kept identical, SEM and TEM (Fig.2d~f) images show the as-obtained products are also hexagonal nanoplates, the morphologies and the dimension of the products have no great changes. These results suggest that the reaction time is not a significant factor during the reaction process except that increasing the yield of the product.

In order to investigate the effect of fluoride source, K_2SiF_6 is used instead of $NaBF_4$ to synthesize LaF_3 by an identical procedure. LaF_3 solids are obtained from the reaction of $La(NO_3)_3 \cdot 6H_2O$ with K_2SiF_6 ($n_{La^{3+}}/n_{SiF_6^{2-}}$=1∶0.5) after 6 h. SEM and TEM images show that only uniform bundles-like morphologies with length of *ca.* 400 nm and width of 200 nm, are observed for these products (Fig.3a ~b). The magnified SEM and TEM images reveal that the surfaces of the bundles are not smooth and made of small nanocrystals (Fig.3c ~d). When the reaction time is prolonged to 12 h, the as-prepared LaF_3 kept the bundle-like morphology as shown in the SEM and TEM images (Fig.3e~f).

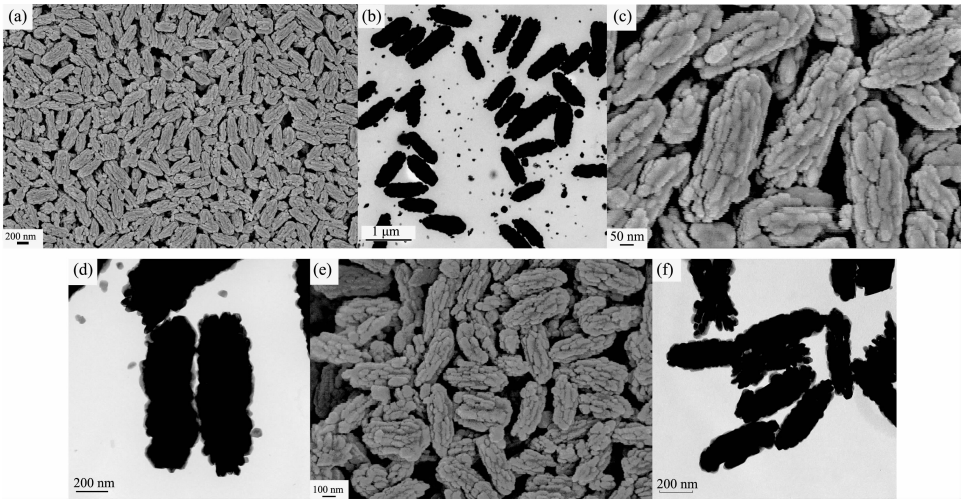

Fig.3 SEM and TEM images of the LaF_3 prepared from K_2SiF_6 ($n_{La^{3+}}/n_{SiF_6^{2-}}$=1∶0.5) in different periods of time: a~d (6 h), e~f (12 h)

2.3 Effect of reaction parameters

To obtain a better understanding of the effect of reaction parameters, a series of experiments are carried out to investigate the detailed information, such as molar ratio of starting materials, reaction time and temperature. Firstly, the molar ratio of reactants is investigated. As shown in Fig.1a, when fixing the molar ratio of $n_{La^{3+}}/n_{BF_4^-}$ as 1∶0.75 and reacting for 6 h, the diffraction peaks of the as-obtained LaF_3 are much sharper than the product from $n_{La^{3+}}/n_{BF_4^-}$=1∶2. Therefore, it is believed that the product crystallinity improves and grain size increases with the increasing of molar ratio of the reactants. The corresponding SEM images of the product ($n_{La^{3+}}/n_{BF_4^-}$=1∶2) are shown in Fig.4a ~b. The morphologies of the as-prepared LaF_3 also exhibit as hexagonal plates, but the edges are not smooth and the size is different from each other. Further increasing the molar ratio of $n_{La^{3+}}/n_{BF_4^-}$ to 1∶4, or 1∶8, respectively, the products are hexagonal plates with similar morphology and size to that sample prepared with the molar ratio of $n_{La^{3+}}/n_{BF_4^-}$ as 1∶2. Meanwhile, varying the molar ratio of $n_{La^{3+}}/n_{SiF_6^{2-}}$ does not have any effect on the crystalline phase of the products. Secondly, as shown in Fig.2 and Fig.3, the time-dependent experiments results indicate that the reaction time has no significant influence on the crystalline phase and the shape of the as-prepared LaF_3. Thirdly, it is noted that the reaction temperature plays no important role in the formation of LaF_3 plates or bundles. In order to validate it, a series of contrastive experiments were conducted to fabricate LaF_3 at 60 ℃

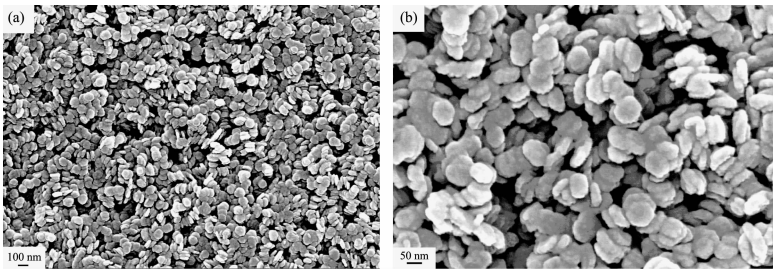

Fig.4　SEM images of the LaF_3 prepared from $NaBF_4$ ($n_{La^{3+}}/n_{BF_4^-}$=1:2) after for 6 h

or 120 ℃ when fixing the molar ratio of $n_{La^{3+}}/n_{BF_4^-}$ as 1:0.75, consequently, the corresponding product is similar in shape and displays as hexagonal nanoplates.

Furthermore, Fig.1a~b show the XRD patterns of 5 mol% Eu^{3+} or Tb^{3+}-doped LaF_3 samples prepared from $NaBF_4$ ($n_{La^{3+}}/n_{BF_4^-}$=1:0.75) and K_2SiF_6 ($n_{La^{3+}}/n_{SiF_6^{2-}}$=1:0.5) after reaction for 6 h are characterized. The average crystallite size calculated from the (111), (302) and (221) diffraction peak using the Scherrer equation is about 25 nm. The broadening of the diffraction peaks indicates that the sizes of the doped LaF_3 nanocrystals synthesized by our approach are at the nanoscale. For the lanthanide contraction effects, the diameter of Eu^{3+} or Tb^{3+} is smaller than La^{3+}, therefore, the doping of Eu^{3+} or Tb^{3+} has no obviously effects on the nanocrystalline nature of the samples, as shown in Fig.1a ~b. The morphologies and dimensions of Eu^{3+} or Tb^{3+}-doped LaF_3 samples are similar with those of pure LaF_3 nanocrystals.

2.4　Possible formation mechanism

$$BF_4^- + 3H_2O \rightarrow H_3BO_3 + 3HF + F^- \quad (1)$$

$$SiF_6^{2-} + 3H_2O \rightarrow 2F^- + H_2SiO_3 + 4HF \quad (2)$$

$$Ln^{3+} + 3F^- \rightarrow LnF_3 \quad (3)$$

The use of $NaBF_4$ and K_2SiF_6 plays a critical role in obtaining LaF_3 crystal structures. The Eqs(**1~3**) have been reported earlier. It is known that $NaBF_4$ (or K_2SiF_6) yields F^- by hydrolysis of BF_4^- (or SiF_6^{2-}), and then F^- ions react with Ln^{3+} to form LnF_3. In the current study, it is obvious that the morphology of LaF_3 can be controllably synthesized by varying the fluoride sources. The detailed formation of mechanism and the unique role of $NaBF_4$ and K_2SiF_6 in determining LnF_3 (Ln =Y, Eu, Sm) structures have been investigated [14,17,20]. $NaBF_4$ and K_2SiF_6 and their decomposed products could be absorbed onto the surfaces of LaF_3 seeds, facilitating the preferential growth of some specific crystalline planes. As a result, LaF_3 nanocrystals with different morphologies (plates and bundles) have been synthesized by varying the fluoride source ($NaBF_4$ and K_2SiF_6).

2.5　Luminescence properties

The room-temperature emission spectra for 5 mol% Eu^{3+} or Tb^{3+}-doped LaF_3 samples, prepared from $NaBF_4$ ($n_{La^{3+}}/n_{BF_4^-}$=1:0.75) and K_2SiF_6 ($n_{La^{3+}}/n_{SiF_6^{2-}}$=1:0.5) in a period of 6 h, are shown in Fig.5. For Eu^{3+}-doped LaF_3, when the samples are exc ited at 397 nm, the

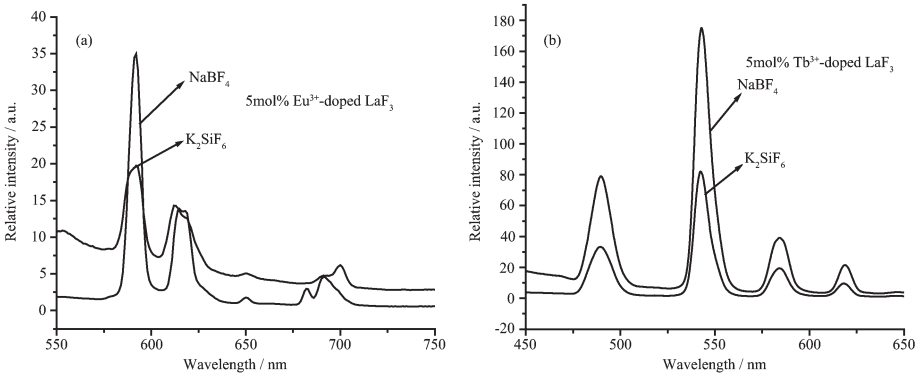

Fig.5　PL spectra of the 5mol% Eu^{3+}-doped LaF_3 (a) and Tb^{3+}-doped LaF_3 (b)

corresponding emission peaks are observed at 592, 615, 651 and 692 (698) nm. They originated from the transitions between the $^5D_0$ excited-state and the ^7F_J (J= 1, 2, 3, 4) ground states of Eu^{3+} ion[16]. Meanwhile, for Tb^{3+}-doped LaF_3, when the samples are excited at 376 nm, the emission spectrum exhibits four well-resolved peaks centered at 490, 543, 584, and 619 nm, corresponding to Tb^{3+} transitions of $^5D_4 \rightarrow {}^7F_J$ (where J = 6, 5, 4, 3)[15]. As shown in Fig.5a~b, although the major peaks in the emission spectra of these samples are identical, the emission intensity is different. Normally, these differences in the PL spectra can be caused by factors such as the extent of crystallinity, morphology, size distribution, homogeneity and dimension of the luminescent material.

3 Conclusions

Via a simple room-temperature solution route, hexagonal phased LaF_3 with different morphologies (nanoplates and bundles) have been synthesized by employing $NaBF_4$ and K_2SiF_6 as fluoride sources. Fluoride sources and molar ratio of reactants play crucial roles on the formation of different morphologies for products. The photoluminescent properties of Eu^{3+} or Tb^{3+} doped LaF_3 crystals have been investigated.

References:

[1] Stouwdam J W, van Veggel F C J M. *Nano Lett.*, **2002**,**2**:733-737

[2] Sivakumar S, Boyer J C, Bovero E, et al. *J. Mater. Chem.*, **2009**,**19**:2392-2399

[3] Lezhnina M M, Jüstel T, Ktker H, et al. *Adv. Funct. Mater.*, **2006**,**16**:935-942

[4] Wang F, Zhang Y, Fan X P, et al. *J. Mater. Chem.*, **2006**,**16**:1031-1034

[5] Zhang Y W, Sun X, Si R, et al. *J. Am. Chem. Soc.*, **2005**,**127**:3260-3261

[6] Wang X, Zhuang J, Peng Q. *Nature*, **2005**,**437**:121-124

[7] Li C X, Yang J, Yang P P. et al. *Chem. Mater.*, **2008**,**20**:4317-4326

[8] Liu C, Chen D. *J. Mater. Chem.*, **2007**,**17**:3875-3880

[9] Hu H, Chen Z G, Cao T Y, et al. *Nanotechnology*, **2008**,**19**:375702(9pp)

[10]Cheng Y, Wang Y S, Zheng Y H, et al. *J. Phys. Chem. B*, **2005**,**109**:11548-11551

[11]LIU Gui-Xia(刘桂霞), SU Rui-Xiang(苏瑞相), WANG Jin-Xian(王进贤), et al. *Chem. J. Chinese Universities*(*Gaodeng Xuexiao Huaxue Xuebao*), **2008**,**29**:461-464

[12]ZHANG Mao-Feng(张茂峰), MENG Jian-Xin(孟建新), SHI Zhao-Pu(时朝璞), et al. *Chinese J. Inorg. Chem.*(*Wuji Huaxue Xuebao*), **2006**,**22**:1883-1886

[13]Wei Y, Lu F Q, Zhang X R, et al. *Mater. Lett.*, **2007**,**61**:1337-1340

[14]Wang M, Huang Q L, Zhong H X, et al. *Cryst. Growth Des.*, **2007**,**7**:2106-2111

[15]WANG Miao(王淼), SHI Yu-Jun(石玉军), JIANG Guo-Qing(江国庆). *Chinese J. Inorg. Chem.*(*Wuji Huaxue Xuebao*), **2009**,**25**:1785-1790

[16]Wang M, Huang Q L, Hong J M, et al. *Cryst. Growth Des.*, **2006**,**6**:1972-1974

[17]Li C X, Yang J, Yang P P, et al. *Chem. Mater.*, **2008**,**20**:4317-26

[18]Zhu L, Liu X M, Meng J, et al. *Cryst. Growth Des.*, **2007**,**7**:2505-2511

[19]Zhu L, Li Q, Liu X D, et al. *J. Phys. Chem. C*, **2007**,**111**:5898-903

[20]WANG Miao(王淼), SUN Tong-Ming(孙同明), SHI Yu-Jun(石玉军). *Chinese J. Inorg. Chem.*(*Wuji Huaxue Xuebao*), **2010**,**26**:274-278